atmosphere

MDPI

Article

Modeling the Spatial and Temporal Variability of Precipitation in Northwest Iran

Mohammad Arab Amiri * and Mohammad Saadi Mesgari

Department of Geographic Information System, Faculty of Geodesy and Geomatics Engineering, K. N. Toosi University of Technology, Tehran 19967-15433, Iran; mesgari@kntu.ac.ir

* Correspondence: mohamadamiri89@yahoo.com; Tel.: +98-912-7199790

Received: 10 November 2017; Accepted: 13 December 2017; Published: 17 December 2017

Abstract: Spatial and temporal variability analysis of precipitation is an important task in water resources planning and management. This study aims to analyze the spatial and temporal variability of precipitation in the northeastern corner of Iran using data from 24 well-distributed weather stations between 1991 and 2015. The mean annual rainfall, precipitation concentration index (PCI), and their coefficients of variation were mapped to examine the spatial variability of rainfall. An artificial neural network (ANN) in association with the inverse distance weighted (IDW) method was proposed as a hybrid interpolation method to map the spatial distribution of the detected trends of mean annual rainfall and PCI over the study region. In addition, principal component analysis (PCA) was applied to annual precipitation time series in order to verify the results of the analysis using the mean annual rainfall and PCI data sets. Results show high variation in inter-annual precipitation in the west, and a moderate to high intra-annual variability over the whole region. Irregular year-to-year precipitation concentration is also observed in the northeastern and northwestern parts. All in all, the highest variations in inter-annual and intra-annual precipitation occurred over the western and northern parts, while the lowest variability was observed in the eastern part (i.e., the coastal region).

Keywords: artificial neural networks; Northwest Iran; precipitation concentration index; precipitation variability; principal component analysis

1. Introduction

Rainfall is an important component of hydrological studies, which has significant impacts on general production potential of a specific region, and studying its spatial and temporal variability is useful for water resources management and regional development [1]. Hence, regional variability analysis of precipitation is an important topic in climatological studies.

Precipitation variability at regional scale can influence human society, ecosystems, agriculture and the environment, and can help in regional resources matching [2]. Due to the sparsity of weather station networks across Iran, only a few studies were undertaken on regional variability analysis of precipitation over the country [3–12]. Dinpashoh et al. [3] applied the principal component analysis (PCA) in association with cluster analysis (CA) to 12 chosen variables recorded by 77 stations in Iran, and classified the country into seven homogeneous rainfall sub-regions. Raziei et al. [4] used data from 140 stations in west of Iran between 1965 and 2000, to analyze the spatial distribution of rainfall, and divided the region into five homogeneous precipitation sub-zones. Darand and Daneshvar [13] applied hierarchical clustering analysis to the outcomes of PCA implemented on the high-resolution gridded dataset, and obtained nine homogeneous sub-zones with different precipitation regimes in Iran. Raziei [14] analyzed monthly rainfall time series of 155 stations across Iran between 1990 and 2014, and obtained eight homogeneous sub-regions with different precipitation variability. There are some other interesting researches in the literature that used other methods for precipitation regionalization

in other countries. For instance, Zhu and Li [15] used the rotated empirical orthogonal function (REOF) to divide China into ten rainfall sub-regions.

Precipitation variability can be analyzed at different temporal scales. Sirangelo et al. [16] employed a stochastic model to explain seasonal effects of daily rainfall exceeding the considered threshold values in southern Italy. De Luca [17] analyzed the spatial and temporal variability of rainfall time series at different temporal scales across the Basilicata and Calabria regions of southern Italy and concluded that the process of rainfall breakdown is stationary for finer temporal resolutions. However, the present research is concentrated on annual, seasonal and monthly precipitation.

In this study, the spatial time series that include the spatial and temporal positions of weather stations in space and time coordinate systems, and the recorded non-spatial values (precipitation) were used. Some rainfall parameters, including annual precipitation, precipitation concentration index (PCI) and their coefficients of variation were used to show the spatial patterns of inter-annual and intra-annual variations of precipitation time series. Geographic Information System (GIS) has also been used for the development of a spatial database, spatial processes, and geo-visualization of the results of analysis [18].

Regarding spatial quantification, many different interpolation methods can be used. The methods can be categorized into global and local interpolators, and exact and approximate interpolators. Another distinction can be made between deterministic, probabilistic and other methods. Inverse Distance Weighting (IDW), Nearest Neighborhood (NN) and triangulation, Polynomial functions (splines), linear regression, and Artificial Neural Networks (ANN) are examples of deterministic methods. These methods generate a continuous surface using the geometric characteristics of point samples. Probabilistic methods, on the other hand, are based on probabilistic theory and allow computing the statistical significance of the predicted values. Optimum interpolation, Simple Kriging, Ordinary Kriging, Co-kriging, Universal Kriging, Residual Kriging, Indicator Kriging, Probability Kriging, Disjunctive Kriging, and Stratified Kriging can be classified as probabilistic methods. Other methods are specifically developed for meteorological purposes and are a combination of deterministic and probabilistic methods (e.g., the MISH method (meteorological interpolation based on surface homogenized data basis)).

ANN method has received increasing interest for generating continuous surfaces from climate data sets. The ANN method does not have any restrictive assumptions about stationarity and is able to handle nonlinear relationships between spatial data [19]. Kajornrit et al. [20] proposed the use of modular ANN to estimate missing monthly rainfall data in northeast Thailand. Paraskevas et al. [21] used an ANN model to estimate the spatial distribution of the mean annual precipitation over the Achaia County, Greece. Consequently, the spatial distribution of precipitation parameters could be investigated using neural networks approach.

A new hybrid method combining the ANN and inverse distance weighted (IDW) approaches was implemented to map the detected trends in annual rainfall and PCI. The ability of handling nonlinear relationships between spatial data, and the lack of pre-assumptions such as stationarity of the input data, are the main advantages of using ANN for interpolation [19]. There are some researches that used soft computing methodologies, including neural networks, support vector regression, genetic algorithm and adaptive neuro-fuzzy inference in climatological applications [6,22,23]. In the present study, the spatial variations of trends of annual rainfall and PCI were mapped using an ANN in association with IDW across the study region.

Principal component analysis (PCA) was used to capture the spatial variability of annual rainfall. The method has some advantages in comparison with other approaches, e.g., its capability to use different combinations of time, objects, and attributes. Richman [24], Dinpashoh et al. [3], Raziei et al. [4], Vicente-Serrano et al. [25], and many other researchers used the procedure in climatological studies.

According to Richman [24], there are six modes of PCA based on different combination of time, objects/entities, and attributes/variables. The aims of the study and the considered variables

can determine which mode of PCA is appropriate for analysis. Serrano et al. [26] claimed that the application of PCA to precipitation time series can be performed in S or T modes. However, there are other studies that utilized other modes of PCA in climate studies, e.g., Raziei et al. [4], and Martins et al. [27]. Consequently, the proper arrangement of data in different types of matrices as input for PCA should be made based on the aims and objectives of the analysis.

In this study, the T-mode PCA was used to capture the spatial variability of precipitation during the considered time period. The T-mode PCA considers the stations as individuals, annual rainfall as constant entity, and observations as variables. Applying the T-mode PCA to the annual rainfall data, the spatial distribution of precipitation time series was investigated and compared with the distribution of mean annual precipitation over the study area. Hence, the difference between interpolating the mean annual rainfall data, and applying the PCA to all the recorded rainfall data instead of aggregated rainfall data (i.e., mean annual rainfall) could be investigated.

The main objective of this research is to assess the inter-annual and intra-annual variability of precipitation. Northwest of Iran was selected to analyze the spatial and temporal patterns in precipitation using data collected at 24 weather stations between 1991 and 2015. By including more than 20% of water resources of Iran, the region is one of the most important hydrological regions of the country; Lake Urmia which is the world's largest hypersaline lakes of the world is also situated in the region [28]. The sub-objectives are: (1) using mean annual rainfall, PCI and their coefficients of variation to envisage the inter-annual, within-year, and year-to-year rainfall concentration; (2) mapping the detected trends in annual rainfall and precipitation concentration using an ANN in association with IDW; and (3) assessing the impacts of using the aggregated rainfall data (mean annual rainfall) and the T-mode PCA for all the recorded precipitation time-series, on the spatial patterns of annual precipitation. The significant level of originality of this study could be exhibited as: (1) analyzing the inter-annual and intra-annual precipitation variability in northwest Iran; (2) introducing a new hybrid interpolation model to map the detected trends of annual rainfall and PCI using only stations with significant trends; and (3) making a comparison between the detected patterns of aggregated and non-aggregated rainfall in the northwest of Iran.

2. Materials and Methods

2.1. Study Area and Rainfall Data

In this study, the northwestern corner of Iran was selected for spatial variability analysis of precipitation. The study area comprised six provinces, namely Ardabil, East Azerbaijan, Gilan, Kurdistan, West Azerbaijan, and Zanjan. The region lies between 43°59′ and 50°41′ East and 34°35′ and 40°2′ North (Figure 1). With a surface area of approximately 169,723 km^2, Lake Urmia inclusive, the region makes up more than 10% of Iran's land area.

In the present study, monthly rainfall time series of 24 weather stations between 1981 and 2015 were used. The spatial distribution of the weather stations is depicted in Figure 1. The data was obtained from the Islamic Republic of Iran Meteorological Organization (IRIMO). The time series have no missing value during the period. The homogeneity of the time series was also analyzed by applying four statistical tests, including the standard normal homogeneity test [29], the Von Neumann ratio test [30], the Pettitt test [31], and the Buishand range test [32].

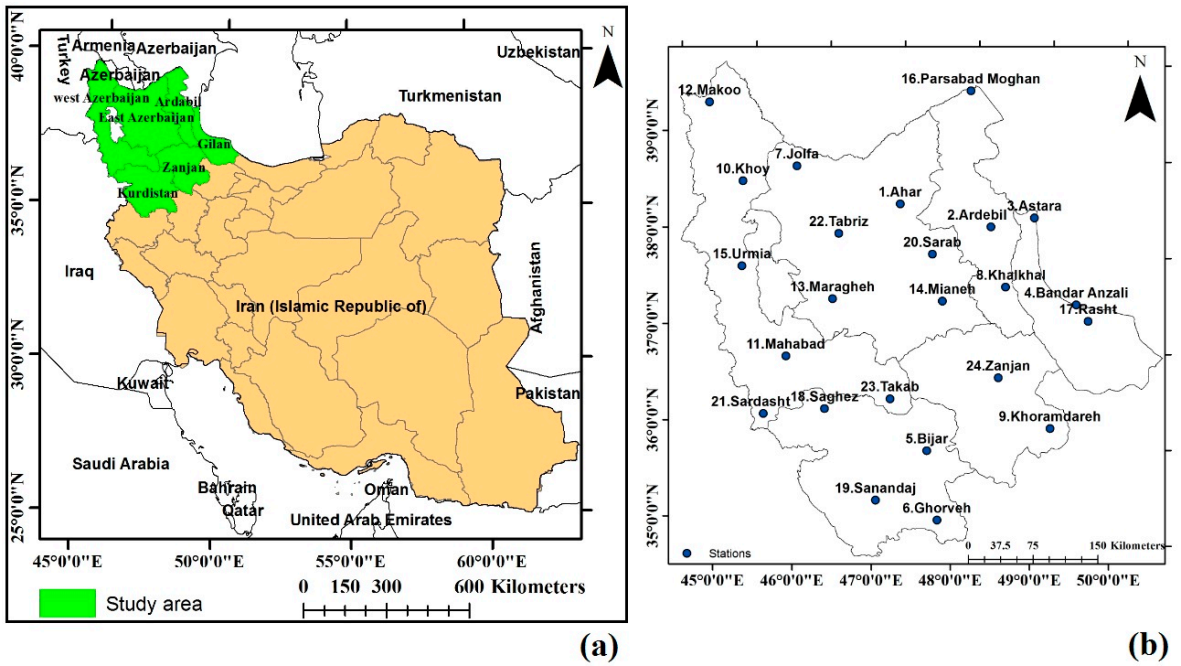

Figure 1. (**a**) The geographic location of the study area; and (**b**) the weather stations used in this study.

2.2. Rainfall Distribution Analysis

The input data were averaged and the values of mean annual precipitation were calculated for all the stations. Then the average values of annual rainfall were interpolated using the Kriging method. In order to show the spatial variability of rainfall in northwest Iran, the coefficient of variation of annual rainfall at each synoptic station was calculated; and then the spatial distribution of the annual rainfall variability was interpolated using the Kriging approach.

The within-year concentration of rainfall can be analyzed using the PCI proposed by Oliver [33]. The following formula is used to calculate the PCI at annual scale:

$$PCI = \frac{\sum_{i=1}^{12} P_i^2}{\left(\sum_{i=1}^{12} P_i\right)^2} \times 100 \quad (1)$$

where P_i is the monthly precipitation in month i.

The degree of seasonality of rainfall can be shown by the PCI. Oliver [33] suggested that the calculated PCI values can be categorized into four classes. According to this classification, the values less than 10, from 11 to 15, between 16 and 20, and greater than 20 represent a uniform, moderate, irregular, and strongly irregular precipitation concentration, respectively [34].

PCI values were calculated for all the 24 weather stations in order to investigate the intra-annual variability of precipitation across the study area. The coefficient of variation of PCI which represents the year-to-year seasonal variability of precipitation was also calculated at each station. Then, the annual PCI and the coefficient of variation of PCI were averaged at each station, and Kriging was used to map the spatial distribution of intra-annual rainfall and inter-annual precipitation concentration in the study area, respectively.

2.3. Trend Analysis and Mapping

Trend of mean annual rainfall and PCI were computed to examine the changing temporal pattern of rainfall over the northwestern corner of Iran between 1991 and 2015. For this purpose, a linear least

square model was used to analyze the trends in annual rainfall and precipitation concentration data. The significance of the calculated trends at each station was tested using student's *t*-distribution.

A multi-layer feed forward neural network was used to obtain trends at un-sampled locations. To train the artificial neural network (ANN) model using the back-propagation algorithm, the latitude, longitude and elevation values (Coordinate System WGS' 84) at each station were used as input parameters, and the computed trends at each station were considered as target parameters. The back-propagation can be formulated as:

$$Y = f(\sum WX + c) \tag{2}$$

where f is a transfer function, which is the rule for mapping the neuron's summed input to its output; W is the weights connecting the input to hidden, or hidden to output nodes; X is the input or hidden node value; Y is the output value of the hidden or output node; and c is the bias for each node.

Leave one out cross-validation technique was utilized to check over fitting properties during the training process. For this purpose, the trend value of an observation station was considered as testing data and the trend values of the remaining stations were used as training data. The training process ends when the mean error computed from the training data is reduced to a pre-defined value.

Two separate neural networks were developed for generating trends of annual rainfall and PCI at un-sampled locations. Having applied the training process, a regular grid was created for every 9 min (0.15 decimal degrees) and the trend values were computed at each point of the constructed grid using the developed ANNs. The three-dimensional coordinates of each grid point were used as input variables, and the trend values of annual rainfall and PCI were considered as outputs of the developed ANN models.

The obtained trend values at each grid point were entered into ArcGIS 10, and the IDW interpolation approach was used to interpolate the obtained trends. It should be noted that the interpolated trend surfaces were generated at which greater weights were assigned to the surrounding eight nearest neighbors in the IDW.

2.4. Principal Component Analysis

PCA is a useful method that was applied to precipitation time series of 24 weather stations in the northwest of Iran. PCA was used in order to find out the independent axes or variances in the precipitation dataset [5]. The method forms new linearly uncorrelated variables called principal components (PCs) that are in a decreasing order of importance [4]. The PCA model can be represented as follows [24]:

$$Z = FA^T \tag{3}$$

where Z is the input data matrix, F is the principal component score matrix, and A is the principal component loading matrix. The data correlation matrix can be defined by the following equation:

$$C = Z^T Z \tag{4}$$

where C is the data correlation matrix.

The following equation is the fundamental principal component (PC) equation in terms of the correlation matrix:

$$C = A \varnothing A^T \tag{5}$$

where $\varnothing$ denotes the principal component score correlation matrix and is an identity matrix under orthogonal rotation.

According to Richman [24], there are six modes of PCA depending on the configuration of input data matrix. In this study, the T-mode PCA was applied to annual precipitation time series. Hence, the stations were considered as individuals (or rows of the input data matrix), and the observations were used as variables (or columns of the input matrix). The co-variability of precipitation time series

were identified by applying the T-mode PCA [4]. For more details on the T-mode PCA, please refer to Richman [24].

The Kaiser's criterion was used to decide on how many PCs should be retained. Having applied the PCA, the retained PCs were rotated using the varimax procedure to maximize the correlation between the obtained PCs and the original variables and to facilitate the interpretation [35]. Then the varimax rotated PC scores were interpolated using the Kriging tool within a GIS across the study region.

3. Results and Discussion

3.1. Statistical Characteristics of Rainfall

The average values of rainfall at all the stations between 1991 and 2015 are presented in Table 1. The mean values of precipitation over northwest Iran vary from 210 mm at Jolfa station to 1662 mm at Bandar Anzali station. Meanwhile, except Bandar Anzali, Astara, Rasht, and Sardasht, which have the four highest values of mean annual rainfall, the values of mean annual precipitation for other stations fluctuate between 200 mm and 450 mm.

Table 1. Mean and standard deviation of annual rainfall and seasonal rainfall at each station.

Station Name	Annual Rainfall		Seasonal Precipitation			
	Mean (mm)	Standard Deviation (mm)	Winter Precipitation (mm)	Spring Precipitation (mm)	Summer Precipitation (mm)	Autumn Precipitation (mm)
1. Aahar	283.44	58.11	70.18	119.55	24.02	69.69
2. Ardabil	286.72	58.92	83.73	99.53	22.83	80.62
3. Astara	1357.61	235.20	293.17	205.40	353.30	505.73
4. Bandar Anzali	1662.00	260.27	335.82	142.32	428.93	754.92
5. Bijar	335.43	74.17	118.06	106.92	9.66	100.79
6. Ghorveh	347.26	74.09	134.41	99.22	8.23	105.39
7. Jolfa	210.01	67.87	42.89	98.83	24.33	43.96
8. Khalkhal	367.70	58.34	106.85	136.77	24.38	99.69
9. Khoramdareh	300.40	82.27	113.27	88.64	7.16	91.32
10. khoy	255.31	54.47	58.93	114.29	27.48	54.61
11. Mahabad	411.17	114.05	161.13	114.15	7.70	128.18
12. Makoo	303.60	70.72	63.58	140.85	43.37	55.80
13. Maragheh	292.47	91.06	99.73	99.97	9.76	83.00
14. Mianeh	274.04	67.14	91.50	91.75	14.34	76.45
15. Urmia	308.60	105.74	100.80	109.99	14.32	83.47
16. Parsabad Moghan	267.93	63.65	64.31	82.02	42.62	78.97
17. Rasht	1306.47	268.16	339.43	169.24	261.88	535.91
18. Saghez	458.34	142.39	189.04	116.41	8.96	143.92
19. Sanandaj	397.56	97.98	162.93	100.84	2.91	130.87
20. Sarab	249.52	42.06	54.10	112.08	29.00	54.33
21. Sardasht	874.25	199.48	395.25	195.50	6.50	278.82
22. Tabriz	245.95	57.10	67.76	101.46	15.04	61.69
23. Takab	318.42	90.41	106.49	107.41	9.50	95.02
24. Zanjan	290.42	65.10	92.25	102.49	16.88	78.79

The seasonal distribution of precipitation at each station from 1991 to 2015 is presented in Table 1. We considered the hydrological year for computing seasonal (cumulated) precipitation, i.e., winter (January, February, March), spring (April, May, June), summer (July, August, September) and autumn (October, November, December) [4]. Generally, the seasonal distribution of rainfall is region specific. For more details, the highest amounts of rainfall at Astara, Bandar Anzali, and Rasht stations that are located in the neighborhood of the Caspian Sea, belong to autumn. In this region, rainfall values in other seasons are also much higher than other stations. While, in general, the other stations have high rainfall values in winter, spring and autumn.

The monthly distribution of rainfall is depicted in Figure 2. To compute monthly precipitation over the whole region, the mean values of monthly total precipitation at all the stations were used. The rainiest months are November, April and March by approximately 13, 12.5 and 11 percentages of total annual precipitation, respectively. In contrast, July, August and June are the driest months by less than three percent of annual rainfall. It is also clear that there is an increasing trend in average

precipitation from January to April. Then, the trend is downward till the end of summer. There is also a dramatic increase in precipitation amounts from August through to November, following by a decline in December. It can be concluded that more than 91% of precipitation occurs during September to May in the northwest of Iran.

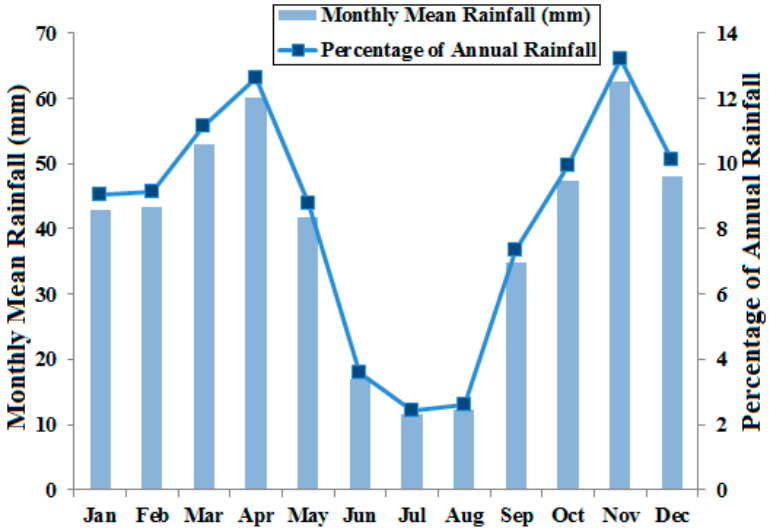

Figure 2. Monthly distribution of rainfall computed over the period 1991–2015.

The seasonal (cumulated) distribution of precipitation over the study area can be calculated using monthly precipitation values and considering hydrological seasons. Autumn with an average amount of precipitation at about 158 mm that constitutes 33% of the total annual precipitation seems to be the wettest season. Winter is also the second rainiest season with the mean precipitation at 139 mm and 29% of annual precipitation. The mean annual rainfall in spring is 119 mm, and a quarter of annual rainfall occurs during this season. The driest season on the other hand is summer, with a mean precipitation of 59 mm, and about 12% of annual precipitation. In summary, approximately 88% of annual total rainfall occurs during autumn, winter and spring.

3.2. Spatial Variability of Rainfall

The interpolated map of mean annual rainfall is shown in Figure 3a. The highest amount of precipitation belongs to the eastern side of the study area, which is located near the Caspian Sea. Rainfall values decrease gradually when moving from east to the central parts of the region. The southwestern corner of the region has also considerable amounts of precipitation. The northern and central parts have the lowest precipitation values in comparison with other parts of the study region. From the produced map, it is clear that precipitation is not distributed monotonically over northwest Iran.

Calculating the coefficient of variation of annual rainfall at each station, the interpolated map of rainfall variability was produced (Figure 3b). Classification of spatial pattern of the inter-annual rainfall variability depends on the precipitation characteristics of a specific region [18]. From the map, it can be seen that rainfall is highly variable in the western part of the region, Lake Urmia inclusive. Thus, the region is highly prone to droughts. Lake Urmia is the world's largest hypersaline lake, and recently experiences a serious desiccation. Tisseuil et al. [28] predicted that if this drying up trend continues until 2100, the Lake level will be reduced three more meters. On the other hand, the inter-annual variability of rainfall is less variable in the coastal regions (eastern side of the region), which have the highest values of precipitation in comparison with other parts of the study area. A moderate variability is also observed in the other parts of the region. In general, the inter-annual rainfall variability gradually decreases from west to east.

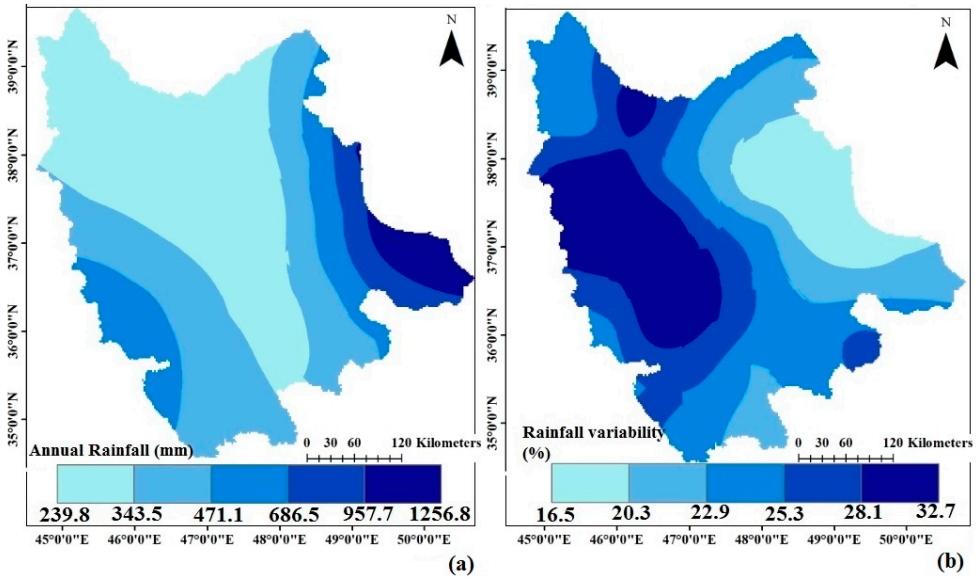

Figure 3. Spatial distribution of (**a**) mean annual rainfall, and (**b**) rainfall variability over the northwestern corner of Iran.

3.3. PCI Variability

Computing the PCI at each station, PCI values were interpolated over the region (Figure 4). The map of PCI shows intra-annual distribution of precipitation, and only allows us to examine the within-year variability of rainfall [18]. According to the classification suggested by Oliver [33], with PCI values between 16 and 20, the central and southwestern parts of the region show irregularity in rainfall distribution; this means that the degree of seasonality of rainfall in this region is high. Moderate precipitation concentration is also observed in other parts of the region. Hence, rainfall is moderately seasonal in eastern and northern parts of the region.

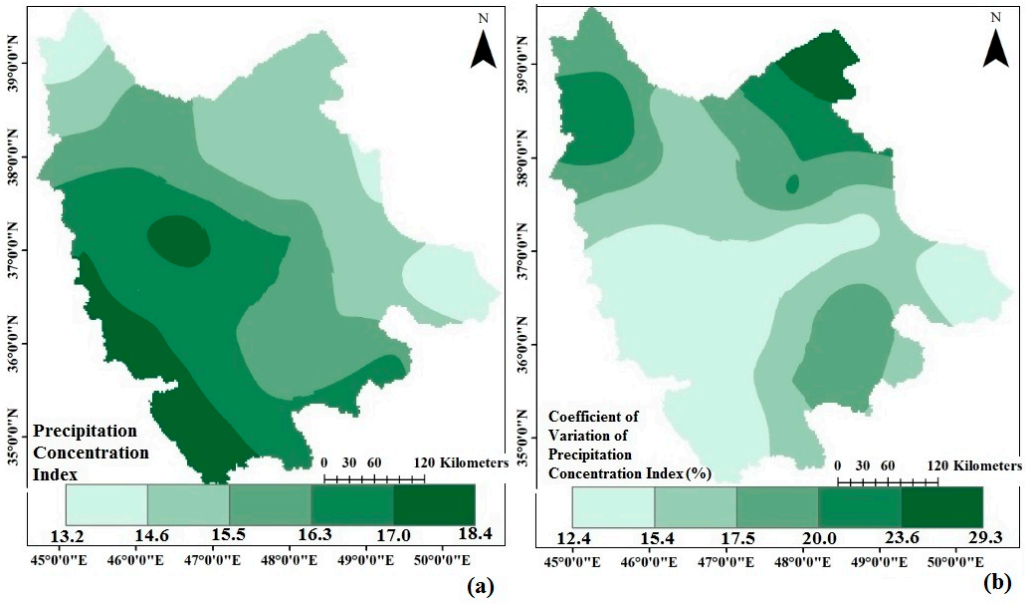

Figure 4. Spatial patterns of (**a**) precipitation concentration index (PCI); and (**b**) Coefficient of variation of PCI.

The map of coefficient of variation of PCI is also produced (Figure 4) in order to show the inter-annual variations of precipitation concentration. The map shows higher values in northeastern and northwestern parts of the region, which means that year-to-year seasonal variability of precipitation is high in these parts. The southern part and especially the southeastern part show the lowest inter-annual precipitation concentration. It is interesting to mention that the southeastern part, which is recognized as the high rainfall zone, has the lowest intra-annual and inter-annual variability of rainfall concentration. In general, rainfall is more seasonal in western and northern parts of the region.

3.4. Trends in Annual Precipitation and PCI

The temporal variability of annual precipitation and PCI of all the 24 stations were examined for trend using a linear least square model (Table 2). Out of 24 stations, significant trends of annual rainfall are observed at only ten stations. Negative trends are observed at nine stations and positive trend is observed at only one station. Among the remaining 14 stations, five stations show positive trends of annual rainfall and nine stations show negative trends. Out of 24 stations, four stations show a significant increase of PCI. Among the remaining stations, nine stations show positive changes and the other 11 stations show negative changes in PCI.

Table 2. Trend of annual rainfall and PCI in 24 stations distributed across northwestern Iran between 1991 and 2015.

Station Name	Annual Rainfall Trend	PCI Trend
1. Aahar	−4.418 ***	0.204 ***
2. Ardabil	−5.015 ***	−0.052
3. Astara	−5.648	0.056
4. Bandar Anzali	0.430	−0.072
5. Bijar	−5.863 ***	−0.036
6. Ghorveh	−3.031	−0.070
7. Jolfa	4.491 ****	−0.007
8. Khalkhal	0.202	0.059
9. Khoramdareh	−5.342 ****	−0.006
10. Khoy	0.488	0.077
11. Mahabad	−8.721 ***	0.180 **
12. Makoo	3.354	−0.001
13. Maragheh	−8.971 *	0.255 **
14. Mianeh	−2.909	0.070
15. Urmia	−5.392	0.076
16. Parsabad Moghan	1.293	−0.082
17. Rasht	−17.404 ****	0.046
18. Saghez	−13.340 **	−0.136
19. Sanandaj	−7.003 ****	−0.073
20. Sarab	−1.889	0.113
21. Sardasht	−11.920	−0.027
22. Tabriz	−3.392	0.200 ***
23. Takab	−5.271	0.040
24. Zanjan	−2.510	0.071

* 99% confidence interval; ** 97.5% confidence interval; *** 95% confidence interval; **** 90% confidence interval.

Since there are a few stations with significant trends of annual rainfall and PCI, two ANNs were applied to the results of trend analysis at stations with significant trends in order to investigate the spatial variations of trends of annual rainfall and PCI. For this purpose, a regular grid for every 0.15 decimal degrees was constructed and two separate multi-layer feed forward neural networks were developed to obtain unknown trends at un-sampled locations. The latitude, longitude and altitude values of stations with significant trends were used as input variables, and the desired trend

at each station was considered as the target variable during the training procedure. Having completed the training process, trends of annual rainfall and PCI were calculated using the developed neural networks for all the points on the generated grid. The properties of the developed neural networks are summarized in Table 3. Then, in order to generate continuous surfaces, IDW was applied to the computed trends considering greater weights for stations with significant trends and their eight nearest grid points.

Table 3. Properties of the developed neural networks and errors obtained from cross-validation of each model.

Model No.	Output Variables	Activation Function		Neurons in Hidden Layer	Learning Rate	Epoch	The Average of ME
		Hidden Layer	Output Layer				
1	Annual rainfall trend	Logarithmic sigmoidal	Pure linear	6	0.01	11	0.69
2	PCI trend	Logarithmic sigmoidal	Pure linear	6	0.01	14	0.073

The spatial distributions of trends of annual rainfall and PCI over the northwestern corner of Iran are depicted in Figure 5. The trend maps are interpolated using trend values of stations with significant trends and the computed trends on the grid points. Hence, the spatial variability of trend of annual rainfall and PCI can be described using the produced trend maps. The spatial pattern of the trend of annual rainfall reveals that annual precipitation has increased in the northwestern part, and decreased in other parts of the region. Southwestern and southeastern parts also show the maximum amounts of decrease of annual rainfall throughout the whole period. The spatial distribution of PCI trend shows a positive trend in all over the study area except in the southwestern region. Maximum positive change of PCI is also observed in the central part of the region, meaning that the highest amount of rainfall variability took place within a year.

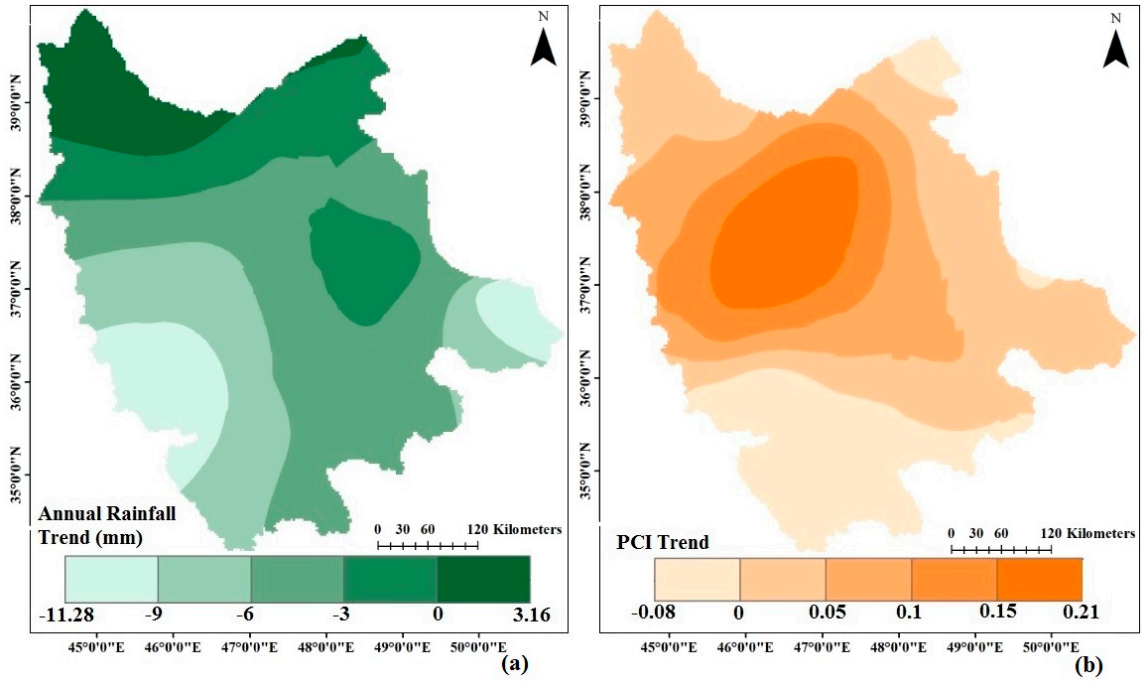

Figure 5. Spatial distribution of trends of (**a**) annual rainfall; and (**b**) PCI over northwest Iran from 1991 to 2015.

3.5. PC Analysis

Applying the PCA to the annual rainfall time series, the retained PCs were rotated by the varimax method (Table 4). The spatial distributions of the first four rotated PC scores over northwest Iran are depicted in Figure 6. The spatial pattern of the first PC score is similar to the spatial patterns of rainfall variability (Figure 3b) and PCI (Figure 4a), delineating the southwestern corner as a distinct region with the highest amounts of values; the values then decline gradually when moving from southwest to northeast. This suggests that the spatial pattern of rainfall variability and PCI can be shown by the first PC score. The second PC score, PC-2, has the highest positive values over the eastern and southwestern parts of the study area, including the regions with higher mean annual rainfall (Figure 3). The PC-3 score shows the lowest values over the southeastern and southwestern parts and the highest values over the northern part, including the regions with the lowest and highest PCI variability (Figure 4b), respectively. The fourth PC score, has also higher values over the northeastern and northwestern parts, depicting the areas with the highest PCI variability (Figure 4b). In summary, the first PC score coincides well with the rainfall variability and PCI maps, and the second PC score refers to the rainy areas in the eastern and southwestern parts (map of mean annual rainfall), while the third and fourth scores coincide relatively well with the map of coefficient of variation of PCI.

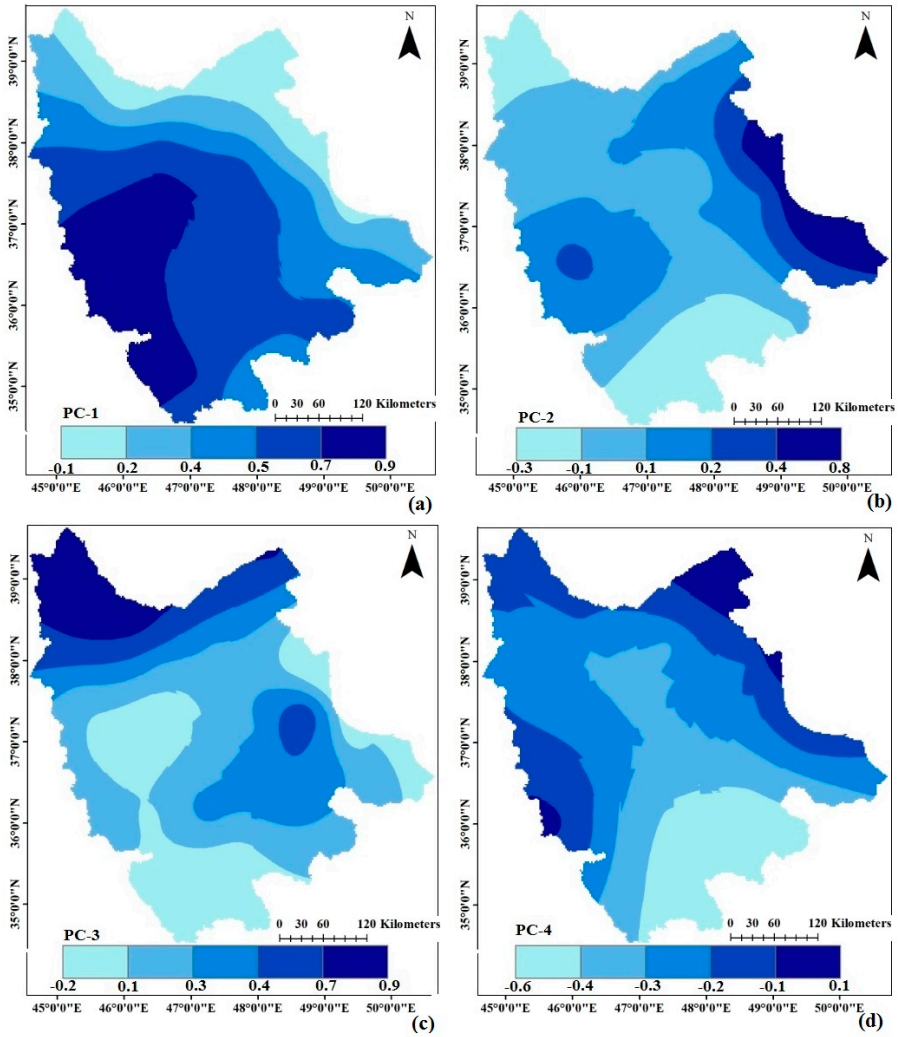

Figure 6. Spatial distribution of Varimax rotated principal component (PC) scores of mean annual rainfall, (**a**) PC-1; (**b**) PC-2; (**c**) PC-3; and (**d**) PC-4.

Table 4. Explained variance (%) by the loadings with and without rotation for total annual precipitation.

Mode of PCA	Explained Variance (%)	Principal Components				Cumulative Percentage of Total Variation
		PC-1	PC-2	PC-3	PC-4	
T-mode PCA	Un-rotated (%)	50.34	13.24	9.34	5.60	78.51
	Varimax rotated (%)	34.55	12.15	14.75	17.06	78.51

Although the previous studies for precipitation variability analysis in Iran were carried out at different spatial and temporal scales using different variables, a comparison can specify whether the obtained results of the present study are in accordance with the results of the previous researches or not. In general, the findings of the previous researches acknowledged the obtained results of the present research. The regionalized map of precipitation by Raziei [14], Darand and Daneshvar [13], and Dinpashoh et al. [3] categorized the southeastern and southwestern parts of the region into two separate clusters, while the central and northern parts were grouped into one homogeneous cluster. Hence, the clustered maps in the mentioned researches are in agreement with spatial patterns of annual rainfall (Figure 3), rainfall variability (Figure 3), coefficient of variation of PCI (Figure 4) and trend of annual rainfall (Figure 5). The clustered map of precipitation by Raziei et al. [4] in the west of Iran only classified the southwestern part as a distinct cluster, and considered other parts of the region in one homogeneous cluster; while the results of the present research showed that the southeastern part of the study region is the rainiest region with the lowest precipitation variability. Thus, it can be concluded that the regionalized map produced by Raziei et al. [4] is not correct, at least in the northwestern part of Iran.

4. Conclusions

Precipitation variability was investigated in the northwest of Iran using monthly, seasonal and annual rainfall time series of 24 weather stations between 1991 and 2015. Mean annual rainfall, PCI, and its coefficients of variation was mapped in order to delineate regions with higher inter-annual and intra-annual precipitation variability. The spatial pattern of the coefficient of variation of mean annual precipitation (the inter-annual variability of precipitation) shows higher variability over the western part of the region. Hence, western part of the region is highly prone to droughts. The minimum inter-annual variation is observed in the coastal region, which has the highest annual precipitation in the study area.

Spatial distribution of PCI reveals a moderate to high precipitation concentration over the whole study region. Intra-annual rainfall distribution reveals more irregularity in the distribution of rainfall in central and southwestern parts of the region. Thus, water related activities such as agriculture are more difficult in these parts. Moderate seasonal variability is also observed in the eastern and northern parts. The coefficient of variation of PCI shows higher values over the northeastern and northwestern parts, which implies that irregular year-to-year seasonal precipitation is mainly concentrated in these regions. Conversely, the lowest intra-annual and inter-annual precipitation variability is concentrated in the high rainfall zone of the study area (i.e., the eastern part).

Temporal trend analysis was carried out to investigate the spatial variation of trends of annual rainfall and PCI. A hybrid interpolation method combining the ANN and IDW was proposed to map trends of annual rainfall and PCI over the region considering greater weights for stations with significant trends and their eight nearest neighbors. The trend analysis of annual precipitation showed an increasing trend over the northwestern part and a decreasing trend in other parts of the study region. Hence, there was a decline in mean annual precipitation in most parts of the region. Furthermore, the results of trend analysis of PCI showed a positive trend in all over the study area except in the southwestern region. Thus, there was a growing trend in the degree of seasonality of precipitation over the study region except the southwestern part.

In order to verify the results of the analysis, the maps of mean annual rainfall, coefficient of variation of mean annual rainfall, PCI, and coefficient of variation of PCI, which were generated using

the mean values of data, were compared with the results of the T-mode PCA. The spatial distributions of the first four PC scores coincide well with the spatial pattern of mean annual rainfall, rainfall variability, PCI, and PCI variability over the northwestern corner of Iran.

Author Contributions: Mohammad Arab Amiri and Mohammad Saadi Mesgari conceived and designed the experiments; Mohammad Arab Amiri performed the experiments; Mohammad Arab Amiri analyzed the data; Mohammad Arab Amiri contributed reagents/materials/analysis tools; Mohammad Arab Amiri wrote the paper.

Conflicts of Interest: The authors declare no conflict of interest.

References

1. Sivakumar, M.; Gommes, R.; Baier, W. Agrometeorology and sustainable agriculture. *Agric. Forest Meteorol.* **2000**, *103*, 11–26. [CrossRef]
2. Alexander, L.; Zhang, X.; Peterson, T.; Caesar, J.; Gleason, B.; Klein Tank, A.; Haylock, M.; Collins, D.; Trewin, B.; Rahimzadeh, F. Global observed changes in daily climate extremes of temperature and precipitation. *J. Geophys. Res. Atmos.* **2006**, *111*. [CrossRef]
3. Dinpashoh, Y.; Fakheri-Fard, A.; Moghaddam, M.; Jahanbakhsh, S.; Mirnia, M. Selection of variables for the purpose of regionalization of Iran's precipitation climate using multivariate methods. *J. Hydrol.* **2004**, *297*, 109–123. [CrossRef]
4. Raziei, T.; Bordi, I.; Pereira, L. A precipitation-based regionalization for Western Iran and regional drought variability. *Hydrol. Earth Syst. Sci.* **2008**, *12*, 1309–1321. [CrossRef]
5. Zoljoodi, M.; Didevarasl, A. Evaluation of spatial-temporal variability of drought events in Iran using palmer drought severity index and its principal factors (through 1951–2005). *Atmos. Clim. Sci.* **2013**, *3*, 193–207. [CrossRef]
6. Arab Amiri, M.; Amerian, Y.; Mesgari, M.S. Spatial and temporal monthly precipitation forecasting using wavelet transform and neural networks, Qara-Qum catchment, Iran. *Arab. J. Geosci.* **2016**, *9*. [CrossRef]
7. Tabari, H.; Somee, B.S.; Zadeh, M.R. Testing for long-term trends in climatic variables in Iran. *Atmos. Res.* **2011**, *100*, 132–140. [CrossRef]
8. Ahani, H.; Kherad, M.; Kousari, M.R.; Rezaeian-Zadeh, M.; Karampour, M.A.; Ejraee, F.; Kamali, S. An investigation of trends in precipitation volume for the last three decades in different regions of Fars province, Iran. *Theor. Appl. Climatol.* **2012**, *109*, 361–382. [CrossRef]
9. Tabari, H.; Abghari, H.; Hosseinzadeh Talaee, P. Temporal trends and spatial characteristics of drought and rainfall in arid and semiarid regions of Iran. *Hydrol. Process.* **2012**, *26*, 3351–3361. [CrossRef]
10. Abolverdi, J.; Ferdosifar, G.; Khalili, D.; Kamgar-Haghighi, A.A. Spatial and temporal changes of precipitation concentration in Fars province, southwestern Iran. *Meteorol. Atmos. Phys.* **2016**, *128*, 181–196. [CrossRef]
11. Arab Amiri, M.; Conoscenti, C. Landslide susceptibility mapping using precipitation data, Mazandaran Province, north of Iran. *Nat. Hazards* **2017**, *89*, 255–273. [CrossRef]
12. Arab Amiri, M.; Mesgari, M.S.; Conoscenti, C. Detection of homogeneous precipitation regions at seasonal and annual time scales, northwest Iran. *J. Water Clim. Chang.* **2017**. [CrossRef]
13. Darand, M.; Daneshvar, M.R.M. Regionalization of precipitation regimes in iran using principal component analysis and hierarchical clustering analysis. *Environ. Process.* **2014**, *1*, 517–532. [CrossRef]
14. Raziei, T. A precipitation regionalization and regime for Iran based on multivariate analysis. *Theor. Appl. Climatol.* **2017**, 1–20. [CrossRef]
15. Zhu, Z.; Li, T. The statistical extended-range (10–30-day) forecast of summer rainfall anomalies over the entire China. *Clim. Dyn.* **2017**, *48*, 209–224. [CrossRef]
16. Sirangelo, B.; Ferrari, E.; De Luca, D. Occurrence analysis of daily rainfalls through non-homogeneous Poissonian processes. *Nat. Hazard. Earth. Syst. Sci.* **2011**, *11*, 1657–1668. [CrossRef]
17. De Luca, D. Analysis and modelling of rainfall fields at different resolutions in southern Italy. *Hydrol. Sci. J.* **2014**, *59*, 1536–1558. [CrossRef]
18. Shahid, S. Spatio-temporal variability of rainfall over Bangladesh during the time period 1969–2003. *Asia-Pac. J. Atmos. Sci.* **2009**, *45*, 375–389.
19. Openshaw, S.; Openshaw, C. *Artificial Intelligence in Geography*, 1st ed.; John Wiley & Sons: Hoboken, NJ, USA, 1997; p. 348.

20. Kajornrit, J.; Wong, K.W.; Fung, C.C. Estimation of missing precipitation records using modular artificial neural networks. In Proceedings of the International Conference on Neural Information Processing, Doha, Qatar, 12–15 November 2012; Huang, T., Zeng, Z., Li, C., Leung, C.S., Eds.; Springer: Berlin/Heidelberg, Germany, 2012; pp. 52–59.
21. Paraskevas, T.; Dimitrios, R.; Andreas, B. Use of artificial neural network for spatial rainfall analysis. *J. Earth Syst. Sci.* **2014**, *123*, 457–465. [CrossRef]
22. Shamshirband, S.; Gocić, M.; Petković, D.; Saboohi, H.; Herawan, T.; Kiah, M.L.M.; Akib, S. Soft-computing methodologies for precipitation estimation: A case study. *IEEE J. Sel. Top. Appl. Earth Obs. Remote Sens.* **2015**, *8*, 1353–1358. [CrossRef]
23. Shenify, M.; Danesh, A.S.; Gocić, M.; Taher, R.S.; Wahab, A.W.A.; Gani, A.; Shamshirband, S.; Petković, D. Precipitation estimation using support vector machine with discrete wavelet transform. *Water Resour. Manag.* **2016**, *30*, 641–652. [CrossRef]
24. Richman, M.B. Rotation of principal components. *Int. J. Climatol.* **1986**, *6*, 293–335. [CrossRef]
25. Vicente-Serrano, S.; Chura, O.; López-Moreno, J.; Azorin-Molina, C.; Sanchez-Lorenzo, A.; Aguilar, E.; Moran-Tejeda, E.; Trujillo, F.; Martínez, R.; Nieto, J. Spatio-temporal variability of droughts in Bolivia: 1955–2012. *Int. J. Climatol.* **2014**, *35*, 3024–3040. [CrossRef]
26. Serrano, A.; García, J.; Mateos, V.L.; Cancillo, M.L.; Garrido, J. Monthly modes of variation of precipitation over the Iberian Peninsula. *J. Clim.* **1999**, *12*, 2894–2919. [CrossRef]
27. Martins, D.; Raziei, T.; Paulo, A.; Pereira, L. Spatial and temporal variability of precipitation and drought in Portugal. *Nat. Hazards Earth Syst. Sci.* **2012**, *12*, 1493–1501. [CrossRef]
28. Tisseuil, C.; Roshan, G.R.; Nasrabadi, T.; Asadpour, G. Statistical modeling of future lake level under climatic conditions, case study of Urmia Lake (Iran). *Int. J. Environ. Res.* **2012**, *7*, 69–80.
29. Alexandersson, H. A homogeneity test applied to precipitation data. *Int. J. Climatol.* **1986**, *6*, 661–675. [CrossRef]
30. Von Neumann, J. Distribution of the ratio of the mean square successive difference to the variance. *Ann. Math. Stat.* **1941**, *12*, 367–395. [CrossRef]
31. Pettit, A.N. A non-parametric approach to the change-point detection. *Appl. Stat.* **1979**, *28*, 126–135. [CrossRef]
32. Buishand, T.A. Some methods for testing the homogeneity of rainfall records. *J. Hydrol.* **1982**, *58*, 11–27. [CrossRef]
33. Oliver, J.E. Monthly precipitation distribution: A comparative index. *Prof. Geogr.* **1980**, *32*, 300–309. [CrossRef]
34. Luis, M.D.; Gonzalez-Hidalgo, J.; Brunetti, M.; Longares, L. Precipitation concentration changes in Spain 1946–2005. *Nat. Hazards Earth Syst. Sci.* **2011**, *11*, 1259–1265. [CrossRef]
35. Santos, J.F.; Pulido-Calvo, I.; Portela, M.M. Spatial and temporal variability of droughts in Portugal. *Water Resour. Res.* **2010**, *46*, 1–13. [CrossRef]